

Cavity cooling of a levitated nanosphere by coherent scattering

Uroš Delić,^{1,*} Manuel Reisenbauer,¹ David Grass,^{1,†} Nikolai Kiesel,¹ Vladan Vuletić,² and Markus Aspelmeyer¹

¹*Vienna Center for Quantum Science and Technology (VCQ), Faculty of Physics, University of Vienna, Boltzmannngasse 5, A-1090 Vienna, Austria*

²*Department of Physics and Research Laboratory of Electronics, Massachusetts Institute of Technology, Cambridge, Massachusetts 02139, USA*

(Dated: April 30, 2022)

We report three-dimensional cooling of a levitated nanoparticle inside an optical cavity. The cooling mechanism is provided by cavity-enhanced coherent scattering off an optical tweezer. The observed 3D dynamics and cooling rates are as theoretically expected from the presence of both linear and quadratic terms in the interaction between the particle motion and the cavity field. By achieving nanometer-level control over the particle location we optimize the position-dependent coupling and demonstrate axial cooling by two orders of magnitude at background pressures as high as 6×10^{-2} mbar. We also demonstrate a significant (> 40 dB) suppression of laser phase noise, and hence of residual heating, which is a specific feature of the coherent scattering scheme. The observed performance implies that quantum ground state cavity cooling of levitated nanoparticles can be achieved for background pressures below 1×10^{-7} mbar.

Laser cooling and trapping is at the heart of modern atomic physics. In its most basic form, motional cooling of atoms [1–3] or molecules [4–8] is provided by the total recoil from both absorption of Doppler-shifted laser photons and the subsequent spontaneous emission. In contrast, coupling the motion of a particle to an optical cavity field can be used for cooling schemes that do not rely on the internal structure of the particle [9, 10]. This is of particular importance for increasingly complex or massive particles, for which transitions between internal energy levels become inaccessible. One highly successful method is to exploit dispersive coupling inside a driven cavity, where the position-dependent cavity frequency shift induced by the particle provides an optomechanical interaction. Demonstrations of this effect include cavity cooling of atomic systems [11–14], as well as the recent experiments in the field of cavity optomechanics that explore the quantum regime of solid state mechanical resonators [15–21]. In the context of levitated nanoparticles [22–25], this cooling scheme is inherently limited by the laser field driving the cavity. Specifically, large drive powers induce co-trapping of the nanoparticle by the cavity field and deteriorate cooling rates [1], while the laser phase noise prohibits ground state cooling at the relevant nanoparticle trap frequencies [2–4, 30].

A promising alternative is cavity cooling by coherent scattering (Fig. 1). In this case, a driven dipole (here: the nanoparticle) produces scattering that is coherent with the drive field (here: the optical trap laser). Scattering of these photons into an initially empty cavity provides a cooling mechanism [31]. As is usual in cavity cooling, the proper red-detuning of the drive field from the cavity allows to resonantly enhance the scattering processes that remove energy from the particle motion. In dispersive coupling schemes the cavity is driven by an external laser such that the particle interaction with the cavity field is determined by the scattering cross-section with

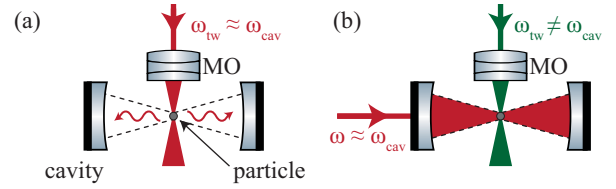


FIG. 1. Different paradigms for cavity cooling of a levitated nanosphere. (a) Cavity cooling by coherent scattering is based on dipole radiation being emitted into an empty cavity, giving the best performance for a particle placed at the intensity minimum of the cavity mode. (b) In standard dispersive optomechanics an external laser drives the cavity. Optimal cooling is at the largest intensity gradient of the cavity mode.

an independently populated cavity mode, which is very small for levitated nanoparticles. In contrast, in coherent scattering a photon can only enter the cavity via the scattering process that cools the particle motion. Efficient cooling originates does not require an additional strong intracavity field, which has the immediate advantage of lifting the above mentioned limitations on drive laser power.

In this Letter we demonstrate cavity cooling by coherent scattering for a levitated dielectric nanoparticle along with its unique features. We report genuine 3D cavity cooling, an effect that has thus far only been demonstrated in 1D with atoms [32, 33]. By positioning the particle with 8 nanometer precision along the cavity axis [1] we can optimize the coherent scattering rates. For a particle placed at a node of the cavity field we observe axial cooling factors beyond 100, limited only by the background pressure and being well described by a simple theory based on linear and quadratic optomechanical interactions. At the same time, we confirm that laser phase noise of the coherently scattered radiation is suppressed by at least four orders of magnitude, which removes a major obstacle for motional ground state cooling

in levitated cavity optomechanics.

Theory. Consider a nanoparticle that is trapped with an optical tweezer of waist W inside an empty optical cavity of mode volume V_{cav} (waist w_0) and at position x_0 along the cavity axis (Fig. 2). The particle interacts with both the optical trap laser and the photons that are coherently scattered off the particle into the cavity. The interaction of the induced dipole with the local electric field is then to first approximation described by the Hamiltonian:

$$H_{dip} = -\frac{\alpha}{2} |\vec{E}_{tw}|^2 - \frac{\alpha}{2} |\vec{E}_{cav}|^2 - \alpha \Re(\vec{E}_{tw} \cdot \vec{E}_{cav}^*). \quad (1)$$

Here α is the particle polarizability, while $E_{tw} \approx \epsilon_{tw} \exp(-(x^2 + y^2)/W^2) \exp(ikz)$ and $E_{cav} = \epsilon_{cav}(\hat{a}^\dagger + \hat{a}) \cos k(x_0 + x)$ are the electric fields of the tweezer in the focal region and the cavity mode, respectively. The cavity and tweezer electric field-per-photon is $\epsilon_{cav} = \sqrt{\hbar \omega_{cav} / (2\epsilon_0 V_{cav})}$ with resonance frequency ω_{cav} and $\epsilon_{tw} = \sqrt{4P_{tw} / (W^2 \pi \epsilon_0 c)}$, while \hat{a}^\dagger (\hat{a}) is the creation (annihilation) operator of the cavity field. ϵ_0 and c are the vacuum permittivity and speed of light.

The first term corresponds to the potential energy of the nanoparticle in the optical tweezer field. The second term describes the dispersive optomechanical interaction of conventional cavity optomechanics experiments that couples the particle to the intensity distribution of the cavity field [21, 34–36]. This interaction is maximized at cavity positions of maximal intensity gradient (i.e. halfway between a node and an antinode of the cavity standing wave). The third term is the interference term between the tweezer and cavity field and represents the coherent scattering interaction that has already been demonstrated in the context of atomic physics experiments [32, 33]. In experiments with levitated nanoparticles the trap laser was far off the cavity resonance, hence this interaction was neglected thus far. Only when the trap laser frequency approaches a cavity resonance, the cavity mode density alters the emission spectrum of the dipole radiation and cavity-enhanced coherent scattering can occur [31]. It has several unique features: First, due to the directionality of the scattered dipole radiation, the interaction strength strongly depends on the polarization of the trap laser. Coherent scattering is driving the cavity through $E_d(\theta) = \alpha \epsilon_{cav} \epsilon_{tw} \sin \theta / (2\hbar)$, where θ is the angle between the polarization axis and the cavity axis. Therefore, a linearly polarized trap laser with $\theta = \pi/2$ maximizes the overlap of the dipole radiation pattern with the cavity mode. Second, the interaction scales with the local field strengths of both optical trap and cavity. For cavities with large mode volume the focused trap laser can significantly boost the interaction strength, specifically by a factor of $\epsilon_{tw} / \epsilon_{cav} \propto w_0 / W$ when compared to the dispersive coupling schemes. Finally, the interaction is linear in the cavity electric field, which then to first

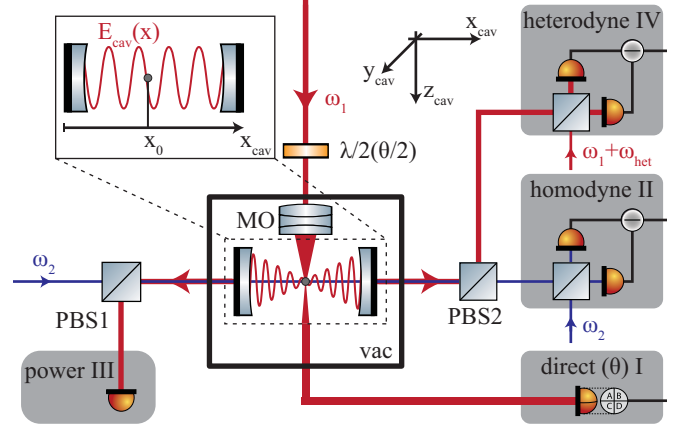


FIG. 2. Setup for 3D cooling by coherent scattering. An optical tweezer is formed by a laser at frequency ω_1 that is tightly focussed by a microscope objective (MO) inside a vacuum chamber (vac). It levitates a nanoparticle at the center of a high-finesse Fabry-Perot cavity. The tweezer linear polarization is set by a half-wave plate ($\lambda/2$). A weak locking beam is derived from the tweezer laser and drives the cavity resonantly at frequency ω_2 , thereby allowing ω_1 and ω_2 to be stably locked relative to the cavity frequency. Four independent detection schemes (I-IV) monitor the particle motion and the cavity field (see main text for details; PBS: polarizing beam splitter; ω_{het} : heterodyne demodulation frequency). Inset: The particle is trapped at a position x_0 relative to a cavity antinode. Maximal coherent scattering occurs for $x_0 = \lambda/4$, i.e. at a cavity node.

order yields the optomechanical interaction

$$\begin{aligned} \frac{H_{CS}}{\hbar} &= E_d(\theta) k \sin kx_0 (\hat{a}^\dagger + \hat{a}) (\hat{x} \sin \theta + \hat{y} \cos \theta) \\ &+ E_d(\theta) \cos kx_0 (\hat{a}^\dagger + \hat{a}) (1 + k\hat{z}). \end{aligned} \quad (2)$$

Here, \hat{x} , \hat{y} and \hat{z} refer to the particle motion with respect to the trap laser polarization axes. Coherent scattering acts as a cavity drive $E_d(\theta)$, with destructive (constructive) interference when the particle is placed at the cavity node (antinode). As a direct consequence, to first order the cavity field does not exert a force on a particle placed in an intensity minimum. Intensity fluctuations of the cavity field as created by phase noise of the drive laser will therefore not result in a fluctuating force. In other words, phase noise heating of standard optomechanical cooling schemes is strongly suppressed when cooling by coherent scattering of the motion along the cavity axis is most efficient [30].

The coupling rates g_x , g_y and g_z from Eq. 2 depend on both polarization (θ) and the particle position (x_0). The optimal position for cavity cooling of the x/y -motion is at the cavity node ($\sin kx_0 = 1$), in stark contrast to cooling via dispersive coupling of standard cavity optomechanics. The scattered light will accordingly consist only of Stokes (heating) and anti-Stokes (cooling) photons, with an imbalance in the scattering rates created by the cavity and leading to an overall cooling of

the x -motion. On the other hand, the z -motion causes a phase shift to the tweezer electric field, which yields maximal coupling along the z -axis at the cavity antinode ($\cos kx_0 = 1$). A proper choice of polarization of the optical trap laser therefore allows to achieve genuine 3D cavity cooling. Further expansion of the dipole interaction includes higher-order optomechanical terms [30].

Experiment. The experimental setup is shown in Fig. 2. A microscope objective (NA 0.8) and a near-confocal high-finesse Fabry-Pérot cavity (Finesse $\mathcal{F} = 73.000$; linewidth $\kappa = 2\pi \times 193$ kHz, length $L = 1.07$ cm, waist $w_0 = 41.1$ μm , resonance frequency ω_{cav}) are mounted inside a vacuum chamber. The microscope objective focuses a 1064 nm laser (frequency $\omega_1 = \omega_{cav} - \Delta$, power $P_{tw} \approx 0.1$ W) to a waist of $W \approx 1.2$ μm , forming an optical tweezer that traps silica nanoparticles (specified radius 71.5 nm). The trap is elliptical in the transverse plane with non-degenerate mechanical frequencies $(\Omega_x, \Omega_y, \Omega_z)/2\pi = (180, 170, 40)$ kHz. To position the particles relative to the optical cavity the microscope objective is mounted on a three-axis nanopositioner with a step size of approximately 8 nm. To precisely control the detuning Δ between the optical trap laser and the cavity resonance frequency, a part of the trap light is frequency shifted to $\omega_2 = \omega_{cav} - \text{FSR} - \Delta$ and weakly pumps the optical cavity (free spectral range $\text{FSR} = 2\pi \times 14$ GHz). It provides a locking signal that enables the source laser for the optical tweezer to follow the freely drifting Fabry-Pérot cavity through a Pound-Drever-Hall locking scheme. Since the locking laser and the optical tweezer are frequency shifted by one free spectral range, they address two different frequency modes of the optical cavity. In other words, the mode populated via coherent scattering of the nanoparticles is initially empty.

The experiment has four detection channels (Fig. 2(b)). Direct detection of the particle motion in all three directions (I) is obtained in forward scattering of the optical tweezer [37]. Homodyne detection of the locking laser in cavity transmission (II) allows for a standard optomechanical position detection along the cavity axis (local oscillator power 0.2 mW). This is used to align the particle with respect to the cavity field without relying on the coherently scattered light. We also directly measure the power of the photons that are coherently scattered into the optical cavity (III) by monitoring the field leaking out of the left cavity mirror. Finally, a spectrally resolved characterization of these photons is enabled by a heterodyne detection of the emission from the right cavity mirror (IV) with a local oscillator of 0.8 mW power and a detuning $\omega_{het}/2\pi = 21.4$ MHz from the optical tweezer frequency.

Polarization dependent cavity cooling. The effect of cavity-enhanced coherent scattering depends on the direction of the dipole scattering off the nanoparticle and hence on the polarization of the optical tweezer. We

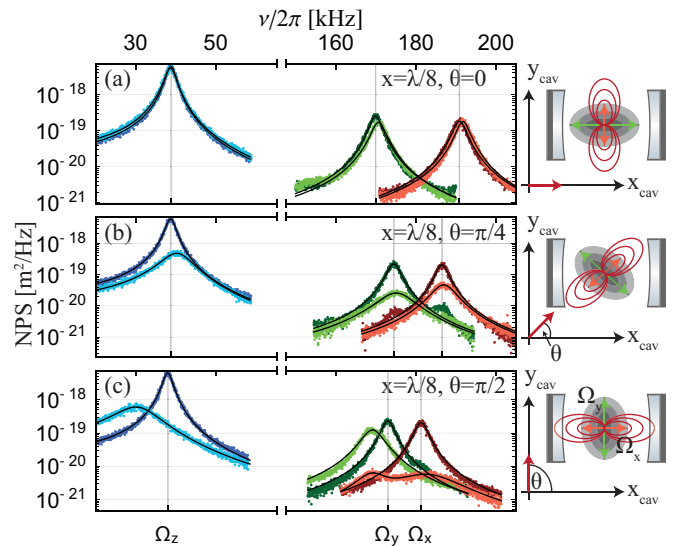


FIG. 3. Polarization-dependent 3D cavity cooling. Shown are noise power spectra (NPS) measured for a particle located at $x_0 = \lambda/8$ away from a cavity antinode and for three different polarizations of the optical tweezer as illustrated on the right panel. The red arrow indicates the polarization. The sketch also indicates the transverse optical tweezer potential (grey ellipse) and the dipole emission (red ellipses), both of which are locked to the tweezer polarization. Noise power spectra in each panel have been obtained along the tweezer axis (z , blue) and in its transverse directions (x , red; y , green). Cooling measurements are performed with a tweezer detuning close to the mechanical frequency ($\Delta = 2\pi \times 300$ kHz, bright color). Measurements at large detuning ($\Delta = 2\pi \times 4$ MHz, dark color), where scattering into the cavity mode is negligible, serve as reference for no cooling (see main text). The nanoparticle was always positioned halfway between the cavity node and antinode to couple all three directions of motion. (a) At $\theta = 0$ no cooling is observed, because polarization along the cavity axis suppresses scattering into the cavity. Imperfect alignment between tweezer and cavity axes results in residual cooling along y - z direction (see main text). (b) At $\theta = \pi/4$ full 3D cavity cooling by coherent scattering is observed, since the cavity axis does not coincide with a principal axis of the optical tweezer. Cooling both broadens the spectra and reduces the overall area. The shift in center frequency is due to the additional optical spring generated by the cavity field. (c) For $\theta = \pi/2$ scattering into the cavity is maximal, as is the cooling along the cavity axis (x) and the tweezer axis (z). Almost no photons are scattered in the third direction (y), resulting in negligible cooling.

investigate cooling by coherent scattering for three linear polarization angles $\theta = 0^\circ$, $\theta = 45^\circ$ and $\theta = 90^\circ$. We record the particle motion using the direct detection (Fig. 2, detection I). As the transverse principle axes of the optical tweezer rotate with the polarization, we also rotate the detection angles to obtain comparable measurements of the amplitude of motion along these axes. For these measurements the particle is positioned on the cavity axis and at the maximum intensity gradient of the empty cavity mode ($x_0 = \lambda/8$) [30] such that cool-

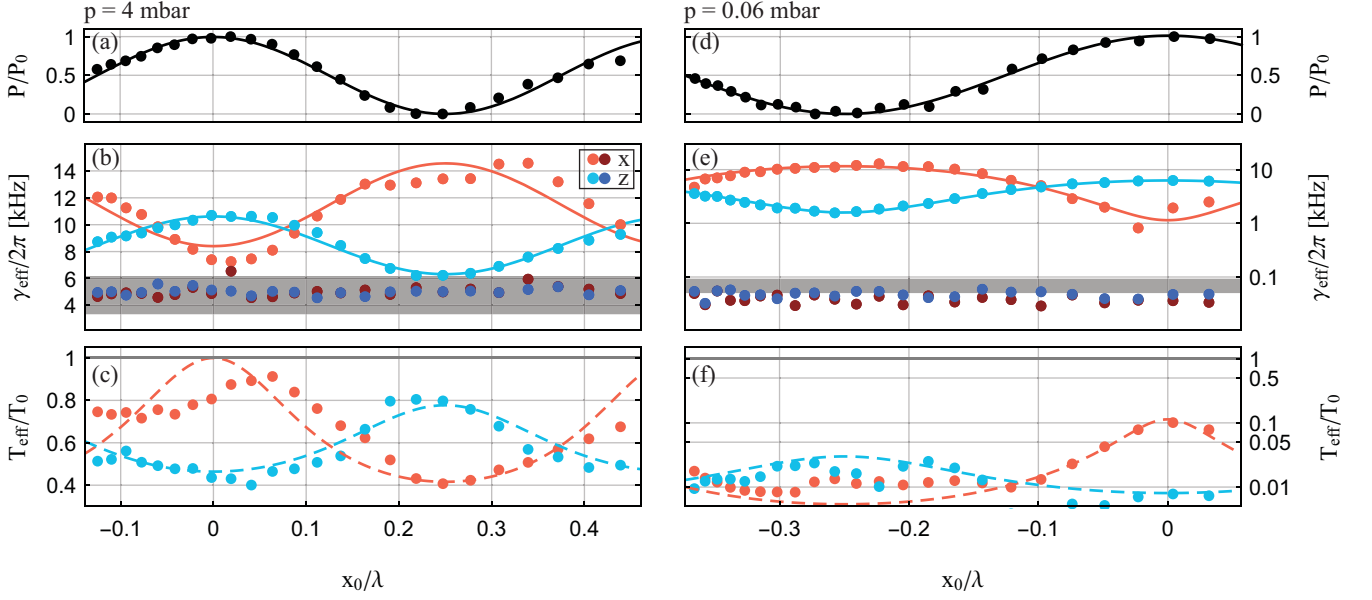


FIG. 4. Position dependent cavity cooling and cooling by quadratic coupling. Shown are relative coherent scattering powers P/P_0 (top), mechanical damping rates γ_{eff} (middle) and inverse cooling factors T_{eff}/T_0 (bottom) for different particle positions x_0 along the cavity axis and at background pressures of $p = 4$ mbar (left) and 6×10^{-2} mbar (right). (top panel; a,d) Coherent scattering into the cavity mode. The black line is a fit to the data following the expected sinusoidal behavior with periodicity $\lambda/2$. The scattering is minimal (maximal) for a particle placed at the node $x_0 = \lambda/4$ (antinode $x_0 = 0$) of the cavity field. (middle panel; b,e) The damping γ_{eff} of the nanoparticle motion is obtained via the width (FWHM) of the mechanical noise power spectra for the x -axis (red) and z -axis (blue). Bright colors indicate measurements with cavity cooling ($\Delta/2\pi = 400$ kHz), dark colors without cooling ($\Delta/2\pi = 4$ MHz). The grey line shows the theoretically predicted gas damping γ_{gas} by the environment, which agrees with the observed damping in the absence of cooling. As expected, maximal damping along the x (z)-direction is obtained for minimal (maximal) coherent scattering powers at $x_0 = \lambda/4$ ($x_0 = 0$). The solid lines are theoretical predictions with no free parameters and agree well with the data for both pressures (see main text). (bottom panel; c,f) The effective mode temperatures T_{eff} are obtained by NPS integration (see main text). As expected, maximum damping implies maximal cooling along both directions. Purely linear coupling would result in vanishing cooling ($T_{\text{eff}}/T_0 = 1$) for locations of minimal scattering, which is not the case for low pressures. Dashed lines represent a theoretical model based on both linear and quadratic coupling without free parameters. The theory agrees well with experimental data, indicating the presence of cavity cooling by quadratic coupling.

ing by coherent scattering affects the axial as well as the transverse motion. For each polarization we compare the cooled motion obtained at a trap laser detuning $\Delta/2\pi = 300$ kHz to an uncooled motion obtained at a much larger detuning $\Delta/2\pi = 4$ MHz.

Initially, we set the trap laser polarization along the cavity axis ($\theta = 0$) by minimizing the scattering into the empty cavity mode (Fig. 3(a)). For perfect polarization alignment a complete suppression of this scattering would be expected. We achieve a suppression by a factor of 100, limited by the alignment between tweezer and cavity axes [30]. The resulting residual coherent scattering is responsible for modest cavity cooling of the y - and z -motion. The x -motion is entirely unaffected as its coupling g_x is smaller by a factor of $\sin \theta$ (see Eq. 2). When the polarization is rotated to $\theta = 45^\circ$ (Fig. 3(b)) all directions of motion are coupled to the cavity mode with rates $(g_x, g_y, g_z)/2\pi = (20, 30, 71)$ kHz, demonstrating genuine 3D cooling by coherent scattering. Rotating the polarization to $\theta = 90^\circ$ (Fig. 3(c)) yields strong cooling

of the x - and z -motion. The observed residual cooling of the y -motion can be explained by a small deviation from the linear trap polarization, which is confirmed by a smaller gap between the mechanical frequencies $\Omega_x - \Omega_y$ compared to $\theta = 0$. The inferred coupling rates in this configuration are $(g_x, g_y, g_z)/2\pi = (42, 16, 94)$ kHz.

Position dependent cavity cooling. We set the polarization angle $\theta = 90^\circ$ to maximize the scattering into the cavity mode. As before, we use the far detuned trap laser ($\Delta/2\pi = 4$ MHz) to calibrate the motion to room temperature. The cooling performance is measured at a detuning of $\Delta/2\pi = 400$ kHz. In order to demonstrate the position dependence of the cavity cooling, we move the particle in steps of ~ 20 nm along the cavity axis at pressures of $p = 4$ mbar (Fig. 4(a)-(c)) and $p = 6 \times 10^{-2}$ mbar (Fig. 4(d)-(f)). The particle position is deduced from the scattered power (detector III, Fig. 4(a) and (d)) and independently confirmed by the homodyne (II) and heterodyne detection (IV) [30]. The maximal effective damping γ_{eff}^x (γ_{eff}^z) of the particle mo-

tion is always observed at the cavity node (antinode), in agreement with destructive (constructive) interference of the scattered photons (Fig. 4(b) and (e)). This is a unique signature of cooling by coherent scattering. We fit the mechanical damping by a simple model $\gamma_{\text{eff}}^{x[z]} = \gamma_{\text{min}} + (\gamma_{\text{max}} - \gamma_{\text{min}}) \sin^2 kx_0 [\cos^2 kx_0]$, yielding the optical linear damping rate $(\gamma_{\text{max}}^{x[z]} - \gamma_{\text{gas}})/2\pi = 10[6.2]$ kHz. Together with independently determined κ , Δ and $\Omega_{x/z}$ it allows us to extract the maximal coupling rates $g_x = 2\pi \times 60$ kHz and $g_z = 2\pi \times 120$ kHz for the respective optimal particle positions. We calculate the cavity drive to be $E_d/2\pi = 2.5 \times 10^9$ Hz, which is a factor of ~ 15 smaller compared to the cavity drive needed to attain an equally large coupling rate g_x by dispersive coupling. We compare the phase noise spectra in the heterodyne detection at the positions of constructive and destructive interference and observe an attenuation of the phase noise by a factor of ~ 50 [30]. Together with the lower requirement on the cavity drive power, this provides us with an estimated suppression of phase noise at the ideal particle position by a factor of $\sim 10^4$ compared to a driven cavity.

We obtain the effective mode temperatures of the x - and z -motion T_{eff}^x and T_{eff}^z from the area underneath the noise power spectra and normalize them to the bath temperature T_0 , i.e. the mode temperatures obtained without cooling (Fig. 4(c) and (f)). At lower pressure both the mechanical damping and the temperature are visibly not reaching the intrinsic values of gas damping (grey line in Fig. 4(b) and (e)) and bath temperature ($T_{\text{eff}}/T_0 = 1$), particularly at positions where cooling by coherent scattering should become negligible. We attribute this to cavity cooling by quadratic interaction, which leads to an average temperature $T_{\text{eff}}^x/T_0^x|_{\text{quad}} = 0.11$ and $T_{\text{eff}}^z/T_0^z|_{\text{quad}} = 0.03$ [5, 30], in good agreement with the experimental data. For comparison, the dashed line in Fig. 4(c) and (f) is based on a theoretical model for the temperatures expected, when both linear and quadratic interaction are included [30].

Conclusion. We have conducted a systematic experimental study of cavity cooling by coherent scattering and shown that the method is superior to dispersive cooling of levitated nanoparticle. As we have demonstrated experimentally, it enables 3D cavity cooling, an effect that has so far only been demonstrated in 1D with atoms [32, 33]. This will make cavity-cooling self-sufficient for experiments in ultra-high vacuum. We have observed cooling to approximately 1 K at a pressure of $p = 6 \times 10^{-2}$ mbar with optical damping rates of up to 10 kHz along the cavity axis in a regime that is far from being limited by self-trapping. We also showed that the position of optimal cooling comes with more than 4 orders of magnitude suppression of laser phase noise heating. Cooling by coherent scattering therefore removes the major obstacles for motional ground state cooling in levitated cavity optomechanics. Given our sideband resolution and

operating the experimental setup in the recoil-limited regime ($p \approx 10^{-7}$ mbar), the expected phonon number would be $\bar{n}_x^{\text{min}} = (\kappa/(4\Omega_x))^2 + \kappa\Gamma_{\text{rec}}/(4g_x^2) = 0.15$ with a ground-state occupation probability of 87%. As a new method for levitated nanoparticles, the coherent scattering as presented here can also enable still stronger coupling rates using higher power in the optical tweezer and larger particles. This opens the path to the regime of ultra-strong coupling where the coupling rate exceeds the mechanical frequency giving rise to novel quantum optomechanical effects [40, 41].

Acknowledgments. This project was supported by the European Research Council (ERC CoG QLev4G), by the ERA-NET programme QuantERA, QuaSeRT (Project No. 11299191; via the EC, the Austrian ministries BMDW and BMBWF and the Austrian research promotion agency FFG), by the Austrian Science Fund (FWF) under Project TheLO (AY0095221, START) and the doctoral school CoQuS (Project No. W1210), and the Austrian Marshall Plan Foundation.

We thank Pablo Solano and Lorenzo Magrini for valuable discussions. We thank the team of Martin Weitz (Tobias Damm) for their help with cutting the cavity mirrors.

Note. We recently became aware of similar work done by Windey et al.

* uros.delic@univie.ac.at

† Present address: Department of Chemistry, Duke University, Durham, North Carolina 27708, United States

- [1] W. D. Phillips, *Reviews of Modern Physics* **70**, 721 (1998).
- [2] H. J. Metcalf and P. van der Straten, *Laser Cooling and Trapping*, Graduate Texts in Contemporary Physics (Springer New York, New York, NY, 1999).
- [3] C. Cohen-Tannoudji and D. Guery-Odelin, *Advances in Atomic Physics*, 1st ed. (World Scientific Publishing Company, 2011) p. 794.
- [4] E. S. Shuman, J. F. Barry, and D. Demille, *Nature* **467**, 820 (2010).
- [5] M. T. Hummon, M. Yeo, B. K. Stuhl, A. L. Collopy, Y. Xia, and J. Ye, *Physical Review Letters* **110**, 143001 (2013).
- [6] J. Lim, J. R. Almond, M. A. Trigatzis, J. A. Devlin, N. J. Fitch, B. E. Sauer, M. R. Tarbutt, and E. A. Hinds, *Physical Review Letters* **120**, 123201 (2018).
- [7] L. Anderegg, B. L. Augenbraun, Y. Bao, S. Burchesky, L. W. Cheuk, W. Ketterle, and J. M. Doyle, *Nature Physics* **14**, 890 (2018).
- [8] D. McCarron, *Journal of Physics B: Atomic, Molecular and Optical Physics* **51**, 212001 (2018).
- [9] V. Vuletić and S. Chu, *Physical Review Letters* **84**, 3787 (2000).
- [10] P. Horak, G. Hechenblaikner, K. M. Gheri, H. Stecher, and H. Ritsch, *Physical Review Letters* **79**, 4974 (1997).
- [11] H. W. Chan, A. T. Black, and V. Vuletić, *Physical Review Letters* **90**, 063003 (2003), quant-ph/0208100.
- [12] P. Maunz, T. Puppe, I. Schuster, N. Syassen, P. W. H.

- Pinkse, and G. Rempe, *Nature (London)* **428**, 50 (2004).
- [13] S. Nußmann, K. Murr, M. Hijkema, B. Weber, A. Kuhn, and G. Rempe, *Nature Physics* **1**, 122 (2005).
- [14] K. M. Fortier, S. Y. Kim, M. J. Gibbons, P. Ahmadi, and M. S. Chapman, *Physical Review Letters* **98**, 233601 (2007).
- [15] S. Gigan, H. R. Böhm, M. Paternostro, F. Blaser, G. Langer, J. B. Hertzberg, K. C. Schwab, D. Bäuerle, M. Aspelmeyer, and A. Zeilinger, *Nature (London)* **444**, 67 (2006).
- [16] O. Arcizet, P.-F. F. Cohadon, T. Briant, M. Pinard, and A. Heidmann, *Nature* **444**, 71 (2006).
- [17] A. Schliesser, P. Del’Haye, N. Nooshi, K. J. Vahala, and T. J. Kippenberg, *Physical Review Letters* **97**, 243905 (2006).
- [18] J. D. Thompson, B. M. Zwickl, A. M. Jayich, F. Marquardt, S. M. Girvin, and J. G. E. Harris, *Nature* **452**, 72 (2008).
- [19] J. D. Teufel, T. Donner, D. Li, J. W. Harlow, M. S. Allman, K. Cicak, a. J. Sirois, J. D. Whittaker, K. W. Lehnert, and R. W. Simmonds, *Nature* **475**, 359 (2011).
- [20] J. Chan, T. P. M. Alegre, A. H. Safavi-Naeini, J. T. Hill, A. Krause, S. Gröblacher, M. Aspelmeyer, and O. Painter, *Nature* **478**, 89 (2011).
- [21] M. Aspelmeyer, T. J. Kippenberg, and F. Marquardt, *Reviews of Modern Physics* **86**, 1391 (2014).
- [22] N. Kiesel, F. Blaser, U. Delić, D. Grass, R. Kaltenbaek, and M. Aspelmeyer, *Proceedings of the National Academy of Science* **110**, 14180 (2013).
- [23] P. Asenbaum, S. Kuhn, S. Nimmrichter, U. Sezer, and M. Arndt, *Nature Communications* **4**, 2743 (2013).
- [24] J. Millen, P. Z. G. Fonseca, T. Mavrogordatos, T. S. Monteiro, and P. F. Barker, *Physical Review Letters* **114**, 123602 (2015).
- [25] P. Z. G. Fonseca, E. B. Aranas, J. Millen, T. S. Monteiro, and P. F. Barker, *Physical Review Letters* **117**, 173602 (2016).
- [1] U. Delić, D. Grass, M. Reisenbauer, N. Kiesel, and M. Aspelmeyer, (unpublished).
- [3] P. Rabl, C. Genes, K. Hammerer, and M. Aspelmeyer, *Phys. Rev. A* **80**, 063819 (2009).
- [4] A. M. Jayich, J. C. Sankey, K. Børkje, D. Lee, C. Yang, M. Underwood, L. Childress, A. Petrenko, S. M. Girvin, and J. G. E. Harris, *New Journal of Physics* **14**, 115018 (2012).
- [2] A. H. Safavi-Naeini, J. Chan, J. T. Hill, S. Gröblacher, H. Miao, Y. Chen, M. Aspelmeyer, and O. Painter, *New Journal of Physics* **15**, 035007 (2013).
- [30] See Supplemental Material at [URL will be inserted by publisher] for the details about the theory, positioning of the particle and data evaluation.
- [31] V. Vuletić, H. W. Chan, and A. T. Black, *Phys. Rev. A* **64**, 033405 (2001).
- [32] M. Hosseini, Y. Duan, K. M. Beck, Y.-T. Chen, and V. Vuletić, *Physical Review Letters* **118**, 183601 (2017).
- [33] D. R. Leibbrandt, J. Labaziewicz, V. Vuletić, and I. L. Chuang, *Physical Review Letters* **103**, 103001 (2009).
- [34] O. Romero-Isart, A. C. Pflanzer, M. L. Juan, R. Quidant, N. Kiesel, M. Aspelmeyer, and J. I. Cirac, *Phys. Rev. A* **83**, 013803 (2011).
- [35] D. E. Chang, C. A. Regal, S. B. Papp, D. J. Wilson, J. Ye, O. Painter, H. J. Kimble, and P. Zoller, *Proceedings of the National Academy of Science* **107**, 1005 (2010).
- [36] S. Nimmrichter, K. Hammerer, P. Asenbaum, H. Ritsch, and M. Arndt, *New Journal of Physics* **12**, 083003 (2010).
- [37] J. Gieseler, B. Deutsch, R. Quidant, and L. Novotny, *Physical Review Letters* **109**, 103603 (2012).
- [5] A. Nunnenkamp, K. Børkje, J. G. E. Harris, and S. M. Girvin, *Phys. Rev. A* **82**, 021806 (2010).
- [39] V. Jain, J. Gieseler, C. Moritz, C. Dellago, R. Quidant, and L. Novotny, *Physical Review Letters* **116**, 243601 (2016).
- [40] C. Genes, A. Mari, P. Tombesi, and D. Vitali, *Phys. Rev. A* **78**, 032316 (2008).
- [41] S. G. Hofer, *Quantum Control of Optomechanical Systems*, *PhD Thesis* (University of Vienna, 2015).

SUPPLEMENTAL MATERIAL

Suppression of scattering by polarization

We observe coupling of both x - and z - motion in the homodyne detection of the locking laser, which is due to a non-straight angle $90^\circ - \varphi$ between the tweezer and the cavity axis [1]. When we set the trap laser polarization $\theta = 0$, the resulting angle between the polarization and the cavity axis is φ . Therefore, the residual scattering into the cavity mode is suppressed by a factor of $\sin^2 \varphi$ compared to the case when $\theta = 90^\circ$. We are able to directly observe the magnitude of suppression of coherent scattering by polarization in the heterodyne detection. We detune the tweezer by $\Delta = 2\pi \times 4$ MHz to avoid affecting the particle motion. By comparing the heterodyne spectra for maximum ($\theta = 90^\circ$) and minimum scattering ($\theta = 0^\circ$) into the cavity mode (Fig. S1), the number of scattered photons is decreased by a factor of ~ 100 , from which we calculate the angle $\varphi \approx 5.7^\circ$. From the ratio of the overall transduction factors in the homodyne detection we obtain a similar value $\varphi \approx 6.3^\circ$, confirming that the seen suppression is consistent with the non-orthogonal tweezer and cavity axes.

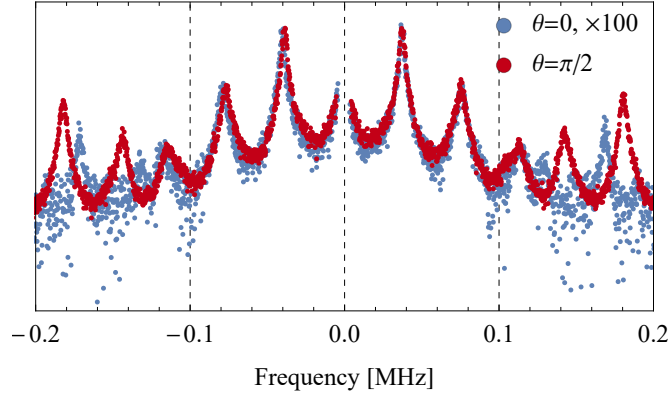


FIG. S1. Overlapped heterodyne measurements for trap laser polarization $\theta = 0$ and $\theta = \pi/2$. Heterodyne measurements are acquired for trap laser far detuned by $\Delta = 2\pi \times 4$ MHz to avoid an affecting the particle motion. Particle is positioned halfway between a cavity node and an antinode ($x_0 = \lambda/8$). The heterodyne spectrum in the case of $\theta = 0$ has been multiplied by a factor of 100 to overlap it with the case of $\theta = \pi/2$. Note that, due to the rotation of the trap axes, we couple x -motion and y -motion for $\theta = \pi/2$ and $\theta = 0$, respectively.

Particle positioning

In the main text, we mainly focus on the enhancement of the coherently scattered light (detector power, III) to determine the particle position x_0 . However, the actual process involves the homodyne detection of the locking cavity mode (homodyne, II) and the heterodyne detection of the scattered photons (heterodyne, IV), which are proportional to the particle x -motion with $g_{lock}^2 \propto \sin^2(2kx_0)$ and $\propto g_x^2 \propto \sin^2(kx_0)$, respectively. This information is used to determine the cavity node and antinode of the cavity mode used for the enhancement of the coherent scattering (Fig. S2). We show that the coupling to the locking mode governed by standard optomechanical interaction (blue) and the coupling in the coherent scattering scheme (green) follow different periodicities in particle position x_0 , as discussed in the main text.

Suppression of the phase noise

The classical phase and intensity noise can influence the lowest reachable phonon occupation in cavity cooling setups [2]. In essence, due to a non-zero detuning of the cooling laser, phase noise is converted into the amplitude and intensity noise in the optomechanical cavity [3]. Phase noise can be implemented into our calculus as a phase variation of the driving field $E_d \rightarrow E_d e^{i\varphi(t)} \approx E_d(1 + i\varphi(t))$, further impacting the particle motion [4]. Phase noise

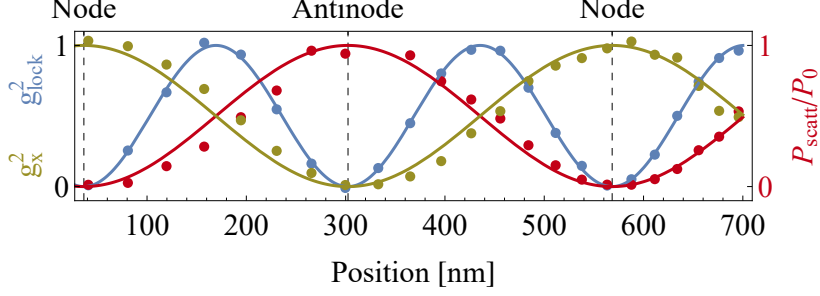


FIG. S2. Positioning of the particle based on different detection schemes. We extract the coupling of the x -motion to the locking cavity mode g_{lock}^2 from the homodyne measurement (blue), demonstrating the standard optomechanical periodicity $g_{lock} \propto \sin(2kx_0)$. Coupling to the cavity mode populated by coherent scattering $g_x \propto \sin kx_0$ is derived from the heterodyne detection (green), where we keep the trap laser far detuned from the cavity resonance by $\Delta = 2\pi \times 4$ MHz in order not to disturb the particle motion. Furthermore, the power scattered out of the cavity (red) is seen out-of-phase with g_x . We are able to reconstruct the nodes and antinodes of the cavity mode used for cavity cooling by coherent scattering.

contribution to the minimum phonon occupation is [3]:

$$n_{min}^{phase} = \frac{n_{phot}}{\kappa} S_{\dot{\varphi}\dot{\varphi}}(\Omega_x) = \frac{E_d^2 \cos^2 kx_0}{\kappa \left(\left(\frac{\kappa}{2} \right)^2 + \Delta^2 \right)} S_{\dot{\varphi}\dot{\varphi}}(\Omega_x), \quad (S1)$$

where $S_{\dot{\varphi}\dot{\varphi}}$ is the laser frequency noise. The calculated cavity drive in the main text for trap laser polarization $\theta = 0$ was $E_d/2\pi = 2.5 \times 10^9$ Hz. In standard optomechanical setup, single photon coupling of x -motion of an equal-sized particle to the cavity mode is $g_0 = 2\pi \times 0.3$ Hz [1], which yields the cavity drive $E_d^M/2\pi = 4.1 \times 10^{10}$ Hz, necessary to reach an equal coupling rate $g_x = 2\pi \times 60$ kHz. Therefore, the suppression of heating from phase noise will be due to the lower required cavity drive E_d and the particle positioning close to a cavity node ($\cos kx_0 \approx 0$). In the experiment we positioned the particle within $\delta x \approx 20$ nm from the cavity node (Fig. S3), which results in the expected total decrease of the phase noise heating by a factor of $(E_d^M/(E_d \cos(\pi/2 + k\delta x)))^2 \approx 1.3 \times 10^4$. More precise positioning is available, with the current nanopositioner step size of 8 nm promising further improvement in the phase noise suppression.

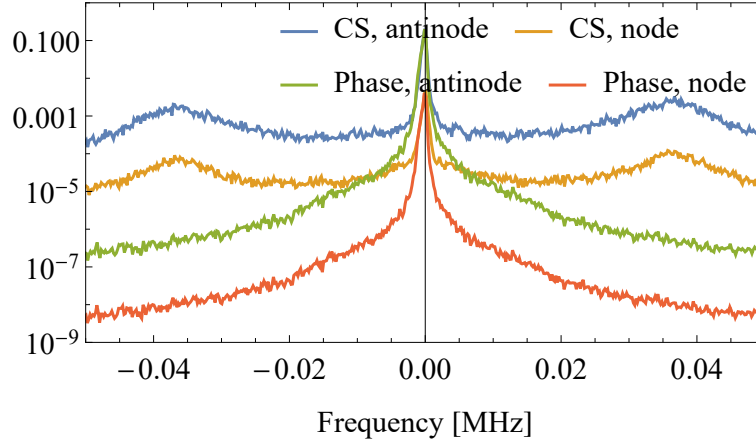


FIG. S3. Phase noise contribution to the heterodyne detection at a cavity node and antinode. Spectrum of the pure phase noise is measured by driving the cavity with an external laser, with the particle placed far from the cavity axis. It is subsequently used to fit the heterodyne spectrum of the coherently scattered photons (blue: particle at an antinode, orange: particle at a node) in the range $(-5, 5)$ kHz at each particle position (green: fit to the blue spectrum, red: fit to the orange spectrum). We observe a decrease of ~ 50 of the phase noise contribution between the antinode and node particle positions. Particle z -motion is observed as well at ~ 40 kHz.

Quadratic cavity cooling

The quadratic coupling rates of the x - and z -motion for the trap laser polarization $\theta = \pi/2$ are:

$$g_{x,\text{quad}} = E_d k^2 x_{zpf}^2 / 2, \quad g_{z,\text{quad}} = E_d k^2 z_{zpf}^2 / 2, \quad (\text{S2})$$

with quadratic cooling rate $\Gamma_{\downarrow,j} = g_{j,\text{quad}}^2 \kappa / |\kappa/2 + i(\Omega_j - \Delta)|^2$, where κ is the cavity decay rate, Δ is the trap laser detuning and Ω_j is the mechanical frequency along $j \in \{x, z\}$ -axis. In the case of $\gamma_{gas} < \Gamma_{\downarrow} n_{th}$, the nonlinear damping due to quadratic cavity cooling leads to a change in phonon number distribution and to an effective cooling [5]. This is valid for the motion along the x -axis for pressures $p \lesssim 4$ mbar. The effective temperature of the particle motion due to the quadratic cavity cooling is:

$$\left. \frac{T_{\text{eff}}}{T_0} \right|_{\text{quad}} = \sqrt{\frac{\gamma_{gas}}{\pi \Gamma_{\downarrow} n_{th}}}, \quad (\text{S3})$$

where $n_{th} = k_B T_0 / (\hbar \Omega_i)$ is the thermal phonon number.

In the main text, we assume a temperature model:

$$\begin{aligned} \frac{T_{\text{eff}}^x}{T_0} &= \frac{1}{T_0} \frac{1}{\frac{\sin^2 kx_0}{T_{\text{lin}}^x} + \frac{\cos^2 kx_0}{T_{\text{quad}}^x}}, \\ \frac{T_{\text{eff}}^z}{T_0} &= \frac{1}{T_0} \frac{1}{\frac{\cos^2 kx_0}{T_{\text{lin}}^z} + \frac{\sin^2 kx_0}{T_{\text{quad}}^z}}, \end{aligned} \quad (\text{S4})$$

which is entirely parametrized by the minimum and maximum temperatures $T_{\text{lin}}^{x[z]}$ and $T_{\text{quad}}^{x[z]}$. We calculate the limit of temperatures in linear cavity cooling from the fit of the effective damping $T_{\text{lin}}^{x[z]}/T_0 = \gamma_{gas}/\gamma_{max}^{x[z]}$.

* uros.delic@univie.ac.at

† Present address: Department of Chemistry, Duke University, Durham, North Carolina 27708, United States

- [1] U. Delić, D. Grass, M. Reisenbauer, N. Kiesel, and M. Aspelmeyer, (unpublished).
- [2] A. H. Safavi-Naeini, J. Chan, J. T. Hill, S. Gröblacher, H. Miao, Y. Chen, M. Aspelmeyer, and O. Painter, *New Journal of Physics* **15**, 035007 (2013), [arXiv:1210.2671 \[physics.optics\]](https://arxiv.org/abs/1210.2671).
- [3] P. Rabl, C. Genes, K. Hammerer, and M. Aspelmeyer, *Phys. Rev. A* **80**, 063819 (2009), [arXiv:0903.1637 \[quant-ph\]](https://arxiv.org/abs/0903.1637).
- [4] A. M. Jayich, J. C. Sankey, K. Børkje, D. Lee, C. Yang, M. Underwood, L. Childress, A. Petrenko, S. M. Girvin, and J. G. E. Harris, *New Journal of Physics* **14**, 115018 (2012), [arXiv:1209.2730 \[physics.optics\]](https://arxiv.org/abs/1209.2730).
- [5] A. Nunnenkamp, K. Børkje, J. G. E. Harris, and S. M. Girvin, *Phys. Rev. A* **82**, 021806 (2010), [arXiv:1004.2510 \[cond-mat.mes-hall\]](https://arxiv.org/abs/1004.2510).